PHYSICAL REVIEW C VOLUME 20, NUMBER 6 DECEMBER 1979

Gamma-ray strength functions for ^{104}Rh, ^{170}Tm, and ^{198}Au

S. Joly, D. M. Drake,* and L. Nilsson†

Service de Physique Neutronique et Nucléaire, Centre d'Etudes de Bruyères-le-Châtel,, B. P. N° 561, 92542 Montrouge Cedex, France

(Received 16 April 1979)

Gamma-ray spectra following neutron capture in rhodium, thulium, and gold for neutron energies between 0.5 and 3.0 MeV have been measured with a NaI scintillator surrounded by an annular NaI crystal. The γ-ray strength functions were deduced from the capture γ-ray spectra by the spectrum fitting method. A bump around 6 MeV is observed for gold as well as a smaller one around 3.5 MeV for thulium. The present results are compared with extrapolations of giant dipole resonance data and measured average total radiative widths.

[NUCLEAR REACTIONS ^{103}Rh, ^{169}Tm, ^{197}Au(n,γ), $E_n = 0.5 - 3.0$ MeV, measured $\sigma(E_n, E_\gamma)$. Deduced γ-ray strength functions. Comparison with other data.]

I. INTRODUCTION

The gamma-ray transition probabilities between low-lying states ($E_\gamma < 2$ MeV) are determined by the conventional techniques of gamma-ray spectroscopy. For transitions of energy greater than about 10 MeV, the probabilities are governed by the properties of the giant resonances. The basic properties of the giant electric dipole resonance are generally well known from photonuclear work. Considerable interest is currently devoted to the study of other giant resonances such as magnetic dipole, isoscalar, and isovector quadrupole.[1] Between the low-energy and the giant resonance regions, the transition probabilities for individual and groups of transitions have been obtained from neutron capture work. However, to get information over a wide region of gamma-ray energies in a single experiment, other methods, e.g., the spectrum fitting method, must be employed.

In the study of the energy dependence of the γ-ray transition probabilities from highly excited states it is usual to introduce a quantity called the gamma-ray strength function. The γ-ray strength function is the distribution, as a function of γ-ray energy, of the average reduced width for a particular multipole type.[2] The γ-ray strength function is an average quantity like the nuclear level density and these quantities are applicable in the same excitation energy region.

The most widely used relationships for the widths of electromagnetic transitions are obtained from the single-particle model[3] which predicts for dipole transitions a strength function independent of E_γ. A more realistic energy dependence of the dipole transition probability is provided by the $E1$ photoabsorption cross section.[4] However, the application of this strength function to describe γ-ray decay between excited states requires an additional assumption. This assumption, known as the Brink hypothesis,[5] states that each excited state has built on it a giant resonance similar to that of the ground state but shifted upwards in energy by the energy of the excited state. With this assumption it is possible to compare the photoexcitation strength function with the γ-decay strength function. From evidence obtained using various methods, the Brink hypothesis seems to be approximately valid. One way to check this hypothesis is to determine whether the energy dependence of the strength function is consistent with the E_γ^5 dependence as given by the Lorentzian shape in the limited energy region of 6 to 8 MeV. The measured γ-ray intensities were found to be in agreement with the extrapolation of the giant dipole resonance for most elements far from closed shells.[2] However, there is definite evidence for significant clustering of electric dipole strength around the unperturbed particle-hole energy for several nuclei, especially below closed neutron shells.

In the present work, the γ-ray strength functions for two nuclei near closed shells (^{104}Rh and ^{198}Au) and one deformed nucleus (^{170}Tm) have been deduced from the capture γ-ray spectra for 0.5 to 3.0 MeV neutrons. The level-density distribution in the residual nucleus has been obtained from other data. The actual spin distribution of the observed low-lying levels has been taken into account in deducing level-density parameters as described in Sec. IV. Accurate knowledge of the γ-ray spectrum shape is of vital importance for this method and special attention was devoted to achieve a high accuracy.

The experimental method presented in the following section was developed to measure neutron

capture cross sections using an NaI spectrometer. Cross sections obtained with this method were found to be in good agreement with previous data obtained with other techniques.[6] Thus we can have confidence in the experimental and data processing procedures used in the present work.

Apart from their interest in fundamental physics, the γ-ray strength functions are used in the calculation of cross sections and γ-ray spectra from capture of fast neutrons. In this respect, more experimental data are needed in order to obtain better systematics of the γ-ray strength function for heavy nuclei.

II. EXPERIMENTAL PROCEDURE AND DATA PROCESSING

The experimental method has been described elsewhere[7] and will be summarized in the present paper. The experimental arrangement is shown schematically in Fig. 1. Neutrons were produced by the ^{7}Li$(p,n)^7$Be and ^{3}H$(p,n)^3$He reactions with the pulsed and bunched proton beam delivered by the 4 MV Van de Graaff accelerator at Bruyères-le-Châtel. The pulse width was about 1 ns and the average proton beam current was typically 4 μA at 1 MHz repetition rate. The air-cooled targets consisted of metallic lithium or tritium adsorbed in titanium on tantalum or gold backings.

The samples were disks 60 mm in diameter and 1.5 mm in thickness for rhodium and gold and 3 mm for thulium. The samples were thin enough to give neutron multiple scattering and γ-ray attenuation corrections smaller than the statistical uncertainties but thick enough to give reasonable count rates. Samples were placed at 73 mm from the target. The neutron energy spread due to the finite solid angle of the sample and the thickness of the lithium (or tritium) target was between 60 and 80 keV depending on the neutron energy.

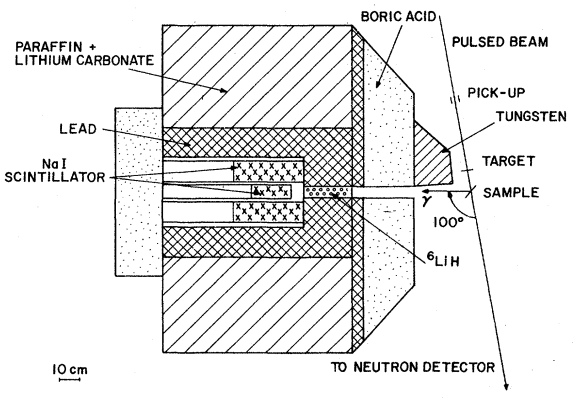

FIG. 1. Experimental arrangement used to record capture gamma-ray spectra.

The gamma rays from the sample were detected by a 76 mm diameter by 152 mm long NaI crystal surrounded by a NaI annulus. The spectrometer was used in anti-Compton (AC) and first-escape (FE) modes simultaneously. The AC pulse-height spectrum contained only pulses not in coincidence with an annulus pulse with energy greater than about 0.1 MeV. In the FE mode, a pulse in the central crystal was recorded only if it was in coincidence with an annulus pulse with energy between 0.25 and 0.75 MeV.

The spectrometer was placed in a heavy shield of paraffin, lithium carbonate, boric acid, and lead. The collimator aperture, 50 mm in diameter, contained a 200 mm long ^{6}LiH cylinder for attenuation of the neutrons scattered by the sample. A tungsten shadow bar was added to shield the γ-ray detector from direct target radiation.

The time-of-flight technique was used to improve the signal-to-background ratio. A fast signal was taken at the anode from the central crystal and sent as a start pulse to a time-to-amplitude converter and the stop signal was generated by the proton beam pulse. Gates were placed on the time spectrum to extract prompt and time-independent pulse-height spectra. It was necessary to record spectra without samples to reject background pulses present in the prompt peak. Figure 2 shows pulse-height spectra obtained with and without the gold sample for 0.72 MeV neutrons. The net pulse-height spectrum is the difference between spectra obtained with and without sample. The net spectrum is grouped into bins 250 keV wide. The neutron flux was measured by a calibrated long counter.[8] For some energies a

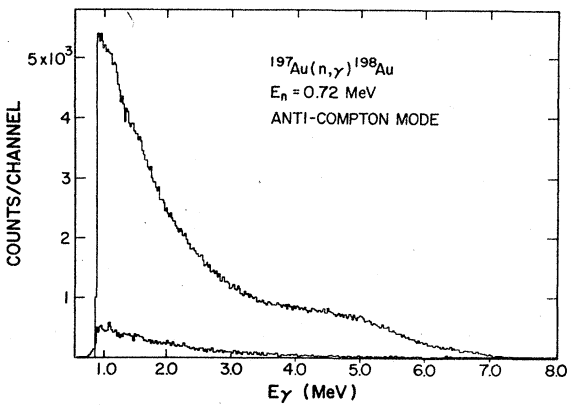

FIG. 2. Gamma-ray pulse-height distributions from the capture of 0.72 MeV neutrons with (upper curve) and without (lower curve) gold sample. The time-independent background has been subtracted and the spectra have been normalized to the same neutron flux.

small plastic time-of-flight scintillator was also used as a monitor.

The spectrum fitting method, used in this work depends on an accurate knowledge of the detector line shape over the whole region of interest. The response functions of the γ-ray spectrometer for the two modes of detection were determined between 1.0 and 12.5 MeV by means of monoenergetic γ rays from radioactive sources and from nuclear reactions. Examples of detector line shapes are given in Ref. 7. Matrices of response functions were constructed from the measured response functions by interpolation in 250 keV steps. To obtain absolute spectral distributions it was necessary to measure the γ-ray efficiency of the spectrometer. Efficiencies were determined using radioactive sources of ^{22}Na, ^{60}Co, and ^{88}Y which had been calibrated to 2.5%. The low-energy efficiencies were extended to higher energies by means of relative intensities of transitions from the ^{11}B$(p,\gamma)^{12}$C and ^{27}Al$(p,\gamma)^{28}$Si reactions. The uncertainty in the γ-ray efficiency curves was estimated to be 3% below 1.8 MeV, increasing linearly to 10% at 12 MeV. The use of the two detection modes presents several advantages. In the AC mode, the total γ-ray efficiency is relatively high for low γ-ray energies and decreases slowly with increasing energy. On the other hand, the FE mode efficiency is low for low-energy γ rays and increases with gamma-ray energy. In fact, the two efficiency curves cross at about 9 MeV. Thus the two detection modes complement each other and the weighted average of the two energy distributions has small uncertainties over the whole energy region.

The gamma-ray energy distribution was obtained by unfolding the net pulse-height spectrum with the spectrometer response matrices.[7] Finally, the unfolded spectrum was corrected for the γ-ray efficiency of the spectrometer and for the γ-ray attenuation in the sample in order to give the capture γ-ray spectrum emitted by the sample.

III. DETERMINATION OF THE GAMMA-RAY STRENGTH FUNCTION

The energy distribution of dipole γ rays emitted by levels at energy U_m can be calculated[9] from the average γ-ray transition probability, or gamma-ray strength function $f(E_\gamma)$, and from the spin independent part of the level-density distribution $\rho_0(U)$:

$$\nu(U_m, E_\gamma)dE_\gamma = 3E_\gamma{}^3 f(E_\gamma)\frac{\rho_0(U_m - E_\gamma)}{\rho_0(U_m)}dE_\gamma . \quad (1)$$

In this expression the strength function for dipole transitions is defined by[2]

$$f(E_\gamma) = \frac{\langle\Gamma(U, E_\gamma)\rangle}{E_\gamma^{\,3}}\rho_0(U) , \quad (2)$$

where $\langle\Gamma(U, E_\gamma)\rangle$ is the average partial γ-ray width for transitions of energy E_γ from states at excitation energy U.

The levels at energy $U_m - E_\gamma$ can deexcite by γ-ray or neutron emission, the process ending when the ground state is reached. The experimentally observed γ-ray spectrum is the sum of primary and subsequent γ rays. The total spectrum is defined by

$$\nu(E_\gamma)dE_\gamma = dE_\gamma \int_{E_\gamma}^{U_m} P(U)\nu(U, E_\gamma)dU , \quad (3)$$

where $P(U)$ is the population density[10] of levels at energy U. The total spectrum calculation was made by dividing the region between the ground state and the initial excitation energy U_m into finite energy intervals[2] of width $\Delta U = 100$ keV. Secondary γ rays from unbound states between $B_n + 0.1$ MeV, where B_n is the neutron separation energy, and U_m have been excluded as the neutron width Γ_n is generally much larger than the radiative width Γ_γ in this energy region.

In the spectrum fitting method, the strength function is obtained by calculating the shape and magnitude of the total γ-ray spectrum with trial functions until good agreement is achieved with the observed spectrum. With the procedure adopted in this work, gamma-ray strength functions are determined between 1.5 MeV and the maximum energy. For comparison with measured total radiative widths [Eq. (4)] the strength function must be extrapolated to zero energy. A constant value or a smooth extrapolation of the shape between 1.5 and 2.5 MeV was used. No information on the low-energy part of the gamma-ray strength function is obtained from the present work because this region of the capture gamma-ray spectrum is masked by gamma rays from inelastic scattering.

The strength functions obtained in this work can be compared with average total radiative widths[2] and with photonuclear data.[4] The average total radiative width $\langle\Gamma_\gamma\rangle$ is related to the γ-ray strength function by

$$\langle\Gamma_\gamma\rangle = \int_0^U 3E_\gamma{}^3 f(E_\gamma)\frac{\rho_0(U - E_\gamma)}{\rho_0(U)}dE_\gamma . \quad (4)$$

The relation between the photonuclear absorption cross section $\sigma_{\gamma a}(E_\gamma)$ and the γ-ray strength function is given by

$$f(E_\gamma) = 8.67\times 10^{-8}\frac{\sigma_{\gamma a}(mb)}{E_\gamma}(\mathrm{MeV}^{-3}) . \quad (5)$$

In deriving the γ-ray strength function all γ rays were assumed to be of the dipole type. The spectrum fitting method is not able to distinguish multipolarities of the γ rays and the strength function is a mixture of the $E1$ and $M1$ strength functions. At high γ energies this empirical strength function represents mainly the $E1$ strength function and can then be compared with the extrapolation of the photonuclear data. However, for lower energies and for some mass regions, the $M1$ transitions have also to be considered but the comparison with the giant dipole resonance (GDR) data is less justified. In some nuclei, collective $E2$ transitions may be important for energies $E_\gamma < 2$ MeV and the deduced γ-ray strength function is to be considered as an effective strength function. The spectrum fitting method has the advantage of providing a strength function over the entire range from near zero to U_m. Moreover, with the procedure used in the present work, it is not necessary to normalize the strength function to the total radiative width at the neutron binding energy. On the other hand, the derived strength function depends on the level-density distribution which is obtained from other sources.

IV. LEVEL-DENSITY DISTRIBUTION

The level-density distribution is given by[11]

$$\rho(U,J) = \rho_0(U)(2J+1)\exp[-J(J+1)/2\sigma^2] . \quad (6)$$

The spin cutoff factor σ was assumed to be energy independent so that in the derivation of Eq. (1), the spin dependent parts of $\rho(U-E_\gamma)$ and $\rho(U)$ cancel. Because the γ-ray strength function is strongly dependent on the level-density distribution, two models, used in the present work, are discussed in this section.

In the back-shifted Fermi gas model (BSFG), the spin independent part of the level-density distribution $\rho_0(U)$ is parametrized by a, the level-density parameter and Δ, a parameter used to account for pairing and shell corrections[12]:

$$\rho_0(U) = \frac{1}{24\sqrt{2}} \frac{\exp[2[a(U-\Delta)]^{1/2}]}{\sigma^3 a^{1/4}(U-\Delta+t)^{5/4}} , \quad (7)$$

where the thermodynamic temperature t is defined by

$$U - \Delta = at^2 - t . \quad (8)$$

The second distribution is given by the constant temperature model:

$$\rho_0(U) = A \exp(U/T) , \quad (9)$$

in which A and T are the parameters.

The two pairs of parameters, a and Δ for the BSFG model and A and T for the constant temperature model, can be found by fitting the functional form of each model to two experimentally determined quantities, the s-wave neutron resonance spacing at the neutron binding energy and the cumulative number of low-lying levels using the procedure described in Ref. 12. We are assuming here that the spin cutoff factor is known. Unfortunately, experimental data on the spin cutoff factor are subject to large errors and σ^2 values corresponding to moments of intertia between 50% and 100% of the rigid-body value $\mathcal{I}_{\text{rigid}}$ have been reported.[13] In the present work, the following expression was used:

$$\sigma_{\text{rigid}}{}^2 = \mathcal{I}_{\text{rigid}} t/\hbar^2 = 0.0150 M^{5/3} t , \quad (10)$$

where M is the mass number of the nucleus. All the relevant parameters for the three nuclei under study are listed in Table I for both $\mathcal{I} = \mathcal{I}_{\text{rigid}}$ and $\mathcal{I} = 0.5\mathcal{I}_{\text{rigid}}$ (method I).

TABLE I. Low-lying level densities, neutron resonance data, and deduced level-density parameters (method I).

		N_0	U_0 (MeV)	D_0 (eV)	B_n (MeV)	I^π	a (MeV^{-1})	Δ (MeV)	A	T (MeV)
^{104}Rh	$\mathcal{I}=\mathcal{I}_{\text{rigid}}$	29 ± 3 [a]	0.54	27 ± 2 [b]	7.00	$\frac{1^-}{2}$	14.445	−1.248	1.302	0.724
	$\mathcal{I}=0.5\,\mathcal{I}_{\text{rigid}}$						12.742	−1.483	2.919	0.801
^{170}Tm	$\mathcal{I}=\mathcal{I}_{\text{rigid}}$	18 ± 2 [c]	0.46	7.3 ± 0.5 [d]	6.59	$\frac{1^+}{2}$	19.473	−0.770	0.565	0.559
	$\mathcal{I}=0.5\,\mathcal{I}_{\text{rigid}}$						17.463	−0.905	1.305	0.609
^{198}Au	$\mathcal{I}=\mathcal{I}_{\text{rigid}}$	17 ± 2 [e]	0.40	16.0 ± 0.2 [f]	6.50	$\frac{3^+}{2}$	17.379	−1.071	0.439	0.617
	$\mathcal{I}=0.5\,\mathcal{I}_{\text{rigid}}$						15.648	−1.233	1.024	0.671

[a] Reference 14.
[b] Reference 15.
[c] Reference 16.
[d] Reference 17.
[e] Reference 18.
[f] References 19, 20.

TABLE II. Low-lying level densities, neutron resonance data, and deduced level-density parameters (method II).

		N_1	U_1 (MeV)	D_0 (eV)	a (MeV^{-1})	Δ (MeV)	A	T (MeV)
^{104}Rh	$g=g_{\text{rigid}}$	14 ± 5 [a]	0.45	27 ± 2 [b]	14.057	−1.543	1.875	0.752
	$g=0.5\, g_{\text{rigid}}$				12.289	−1.889	4.526	0.844
^{170}Tm	$g=g_{\text{rigid}}$	16 ± 3 [c]	0.75	7.3 ± 0.5 [d]	18.977	−1.008	1.039	0.590
	$g=0.5\, g_{\text{rigid}}$				17.316	−0.987	1.708	0.625
^{198}Au	$g=g_{\text{rigid}}$	16 ± 2 [e]	0.42	16.0 ± 0.2 [f]	15.910	−1.960	1.671	0.707
	$g=0.5\, g_{\text{rigid}}$				14.758	−1.836	2.370	0.735

[a] Reference 14.
[b] Reference 15.
[c] Reference 16.
[d] Reference 17.
[e] Reference 18.
[f] References 19, 20.

It has recently been pointed out[21] that low-lying levels with higher spin are difficult to populate and may not have been observed. Therefore, it would be preferable to utilize in the derivation of level-density parameters the cumulative number of levels of a set of particular spins rather than the number of levels with all spins.

In computing the cumulative number of levels, the population of levels having a given spin J is assumed to follow the distribution

$$g(J) = (2J+1)\exp[-J(J+1)/2\sigma^2]\,. \tag{11}$$

In that case the cumulative number N_0 of all levels from $U=0$ to U_0 is given by

$$N_0 = \int_0^{U_0} \rho_0(U) \sum_J g(J)dU \approx \int_0^{U_0} \rho_0(U) 2\sigma^2 dU\,. \tag{12}$$

In an effort to avoid missing levels, we can alternatively consider levels populated by thermal neutron radiative capture, i.e., those being reached by dipole transitions from the capturing states. This choice reduces the actual spin distribution to the interval

$$J_1 = \max(0, I-\tfrac{3}{2}) \leq J \leq J_2 = I+\tfrac{3}{2}\,,$$

where I is the spin of the target nucleus. In this case the cumulative number of levels is given by

$$N_1 = \int_0^{U_1} \rho_0(U) \sum_{J_1}^{J_2} g(J)dU\,. \tag{13}$$

Introducing this method of deducing level-density parameters gives us a total of four ways to calculate level densities, two models and two methods of determining parameters. In Table II are quoted the parameters for both models using the spin selection method [Eq. (13)]. This latter method seems to be the preferred way to count levels and is used throughout the rest of this paper.

The influence of the level-density distribution on the deduced γ-ray strength functions has been studied for gold at 0.5 MeV neutron energy where the capture cross section is large and the statistical uncertainty comparatively small. Deduced γ-ray strength functions for both BSFG and constant temperature formulas are presented in Fig. 3. The curves are very close between 2 and 5.5 MeV but differ by 6% at 1.5 MeV and by 13% at 6 MeV. The effect of the temperature is also shown in Fig. 3. At $E_\gamma = 6$ MeV, a 4% increase in temperature from 0.71 to 0.74 MeV decreases the strength function by about 13%.

Experimental studies[22] show that the BSFG mod-

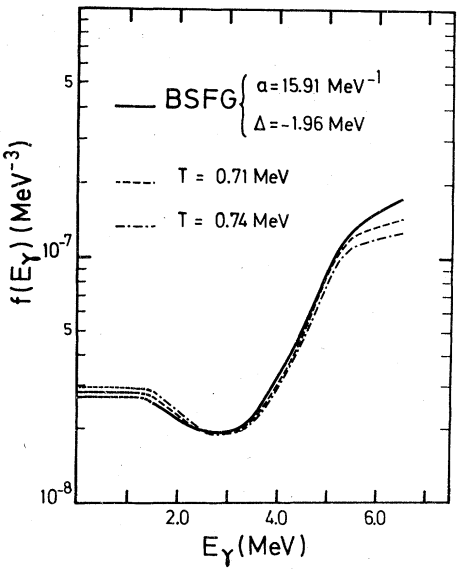

FIG. 3. Gamma-ray strength functions for gold using various level-density distributions.

el reproduces reasonably well level densities for nuclei away from closed shells but that a constant temperature level density works better for closed-shell nuclei. As the gamma-ray strength functions deduced with the two level-density distributions are very similar except at high energies, the constant temperature formula was used in deducing the gamma-ray strength function. A further argument for this choice is that previous works used this distribution facilitating comparisons.

Uncertainty in the level density introduces the largest uncertainty in the strength functions. Other uncertainties are related to limited statistical accuracy in the pulse-height spectra and to limitations in the unfolding procedure but these are generally small compared to that associated with the level-density distribution.

V. RESULTS AND COMPARISON WITH PREVIOUS DATA

The capture γ-ray spectra emitted at 100° are presented in Fig. 4 for neutron energies between 0.5 and 3.0 MeV for gold, rhodium, and thulium. Each spectrum represents the weighted mean of the spectra obtained by the two detection modes. The errors are then weighted errors taking into account efficiency uncertainties and statistical errors. The γ-ray strength functions have been deduced at the neutron energies of 0.52, 0.72, 1.0, 2.0, and 3.0 MeV for the anti-Compton and first-escape detection modes. Thus, ten strength functions were obtained for each element and they were found to be in agreement within 15% for the absolute value and closely similar in shape between 1.5 and 6.5 MeV. The spectra from capture of low-energy neutrons give precise information on the gamma-ray strength functions due to the good statistics. On the other hand, the spectra from capture of energetic neutrons give information at higher gamma-ray energies but the statistical errors are large and consequently, strength functions at high energies are subject to large uncertainties. Another advantage of recording γ-ray spectra at different neutron energies is that possible structures in the strength functions cannot be associated with local irregularities in the level density of the final nucleus. The γ-ray strength function in gold has been studied previously by several groups. Therefore, our results for this nucleus will be presented first.

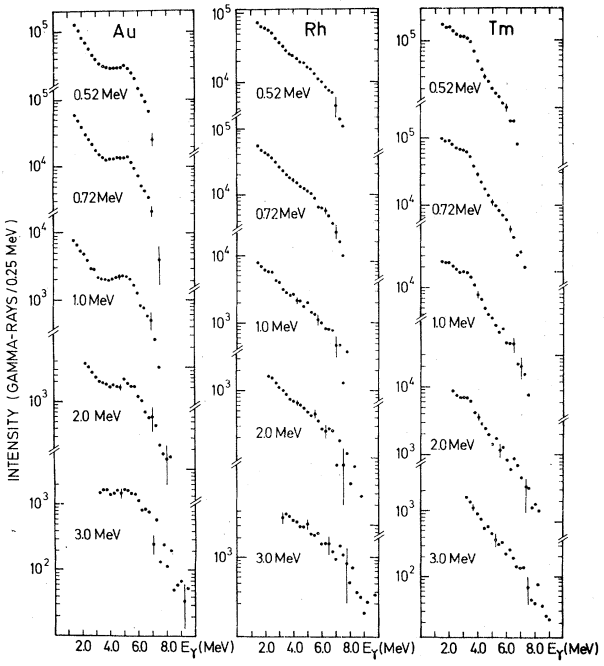

FIG. 4. Capture gamma-ray spectra of gold, rhodium, and thulium for neutrons between 0.5 and 3.0 MeV. The spectra are weighted means of spectra obtained in the AC and FE modes of the γ-ray spectrometer. The error bars represent statistical and γ-ray efficiency contributions.

A. Gold

All the gold capture γ-ray spectra of Fig. 4 show a bump around 5.5 MeV as observed in previous works.[23-26] The average γ-ray strength function for ^{198}Au deduced from the present work is presented in Fig. 5 for $T = 0.71$ MeV and $T = 0.74$ MeV. Because the true level density is expected to be given by a temperature between 0.71 and 0.74 MeV, the γ-ray strength function for ^{198}Au should be in the hatched region between the two curves. Although the maximum γ-ray energy is about 9.5 MeV for 3 MeV incident neutrons, it was not possible to extract a strength function for $E_\gamma > 8.0$ MeV because of the poor statistical quality of the data in this region. As a consequence of unfolding uncertainties, it was not possible to determine the strength function below $E_\gamma = 1.5$ MeV even though the experimental bias was about 0.9 MeV.

Our results are compared with strength functions derived from other experiments using the same or other techniques.

Lundberg and Starfelt[23] measured the γ-ray spectra emitted in the capture of neutrons of energies between 0.03 and 4.2 MeV. The shape of the capture spectrum was found to vary slowly with neutron energy and both spectrum shape and neutron energy dependence are in agreement with the present results. In order to reproduce the experimental spectrum shape, a strength function with a peak at 5.5 MeV was introduced and added

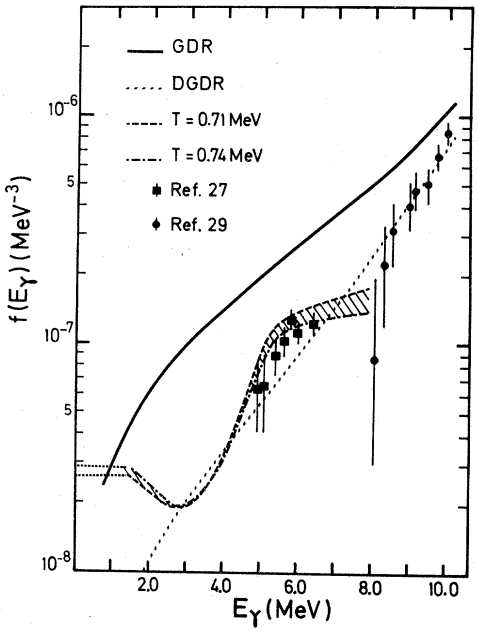

FIG. 5. The ^{198}Au strength function deduced from the present work is represented by the hatched region. Filled circles are photonuclear data and the solid and dotted curves are extrapolations of the Lorentzian and depressed Lorentzian, respectively. The resonance average data are represented by filled squares.

to the Lorentzian shape of the giant dipole resonance. The agreement is reasonable except for energies above 6 MeV where a strength function with a less pronounced minimum around 7.5 MeV would have given a better fit. The level density was represented by the constant temperature formula with $T = 0.6$ MeV.

The thermal neutron capture spectrum was obtained by Groshev *et al.*[24] using a magnetic Compton spectrometer. The spectral distribution shows two groups of transitions around 4.8 and 6.2 MeV, the latter group having the largest intensity. This spectrum is in agreement with fast neutron capture spectra showing a bump between 4 and 6.5 MeV.

The spectrum fitting method has also been used by Earle *et al.*[25] The experimental conditions were different from those of the present work. The NaI detector was shielded only against direct target radiation. The relatively low signal-to-background ratio of the experiment might be at least partly responsible for the intensity excess of gamma rays above 5 MeV in the $E_n = 2.6$ MeV experiment. The level density was represented by the constant temperature formula with $T = 0.75$ MeV.

Earle, Bergqvist, and Nilsson[26] measured the gamma-ray spectra at several neutron energies between 0.03 and 2.5 MeV. Except for the use of a large NaI crystal, the experimental conditions were similar to ours and the capture spectra have about the same shape. The difference between the deduced γ-ray strengths is caused mainly by a slightly different treatment of level densities. In both analyses the constant temperature level-density formula was used with $T = 0.75$ MeV in Ref. 26 and $T = 0.71$ and 0.74 MeV in the present work. The strength function of Ref. 26 was normalized to high-resolution γ-ray results.[27] The γ-ray strength functions deduced from these data[23-26] by the spectrum fitting method are compared to our results in Fig. 6.

Besides the spectrum fitting method, the sequential extraction method has been used to deduce γ-ray strength functions for ^{198}Au. By the $(d,p\gamma)$ reaction[28] a large excitation energy region is populated. In the analysis of the γ-ray spectrum from a particular energy region, it is possible to extract the primary spectrum because the shape of the secondary and subsequent spectra are measured simultaneously. The deduced γ-ray strength function is compared to our data in Fig. 6.

Another way to obtain γ-ray strength function information is to observe primary γ-ray transitions averaged over many resonances.[2] This has

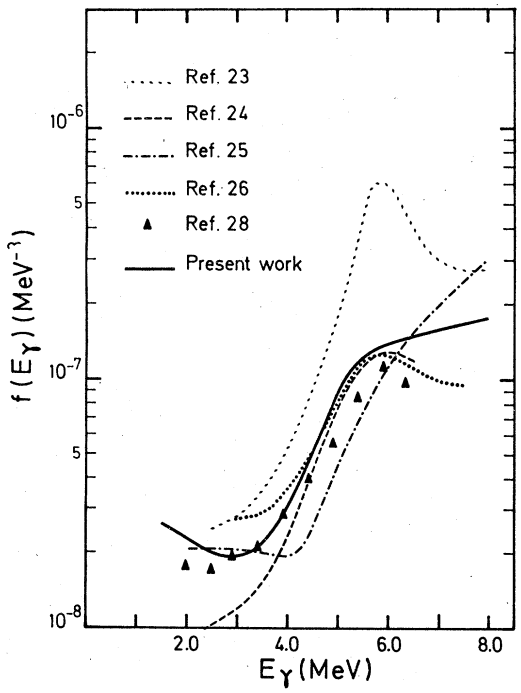

FIG. 6. Comparison of gamma-ray strength functions for ^{198}Au obtained in previous works using the spectrum fitting and the sequential extraction methods.

TABLE III. Giant dipole resonance parameters.

	σ_1 (mb)	E_1 (MeV)	Γ_1 (MeV)	σ_2 (mb)	E_2 (MeV)	Γ_2 (MeV)
^{103}Rh [a]	191	16.15	7.4			
^{nat}Er [b]	225	12.0	2.9	260	15.45	5.0
^{175}Lu [b]	230	12.35	2.7	280	15.52	4.5
^{197}Au [c]	540	13.70	4.75			

[a] Reference 31.
[b] Reference 35.
[c] Reference 29.

been done by Loper *et al.*,[27] who measured the γ-ray spectra of the ^{197}Au$(n,\gamma)^{198}$Au reaction for both thermal and resonance neutrons. The γ-ray strength was deduced from the average intensity of transitions from many resonances to various final states for E_γ between 4.9 and 6.4 MeV. The deduced strength function is compared to our results in Fig. 5. In the same work, the gold γ-ray spectra were compared with spectra from the ^{181}Ta$(n,\gamma)^{182}$Ta reaction which are not expected to have a bump. The γ-ray strength functions for the two nuclei were found to have a giant resonance shape and to be equal within 30%. These data are in agreement with our results within the studied energy region. However, it would be necessary to determine the strength function down to 3.0 MeV and to improve the accuracy of the data in order to observe the anomaly in the ^{197}Au$(n,\gamma)^{198}$Au reaction. The agreement with the E_γ^5 energy dependence could be fortuitous as the deficiency of strength compared to the extrapolation of the giant dipole resonance is compensated by the presence of the 5.5 MeV resonance.

The γ-ray strength function can also be obtained from the photoabsorption cross section $\sigma_{\gamma a}$ according to Eq. (5). Within a few MeV above the neutron separation energy we can set $\sigma_{\gamma a} = \sigma_{\gamma n}$. The giant dipole resonance parameters of Veyssière *et al.*[29] are given in Table III and the data points are plotted in Fig. 5 along with the curve corresponding to the Lorentzian (GDR) used to describe the photonuclear data. The curve is in disagreement with the data points below 12 MeV. A better fit can be obtained down to 8.5 MeV using a Lorentzian shape multiplied, for $E_\gamma < E_0$, by a depression factor of the form

$$\exp[\alpha(E_\gamma - E_0)] . \tag{14}$$

The values $\alpha = 0.164$ MeV^{-1} and $E_0 = 12.2$ MeV deduced by Earle *et al.*[26] were used and the corresponding strength function (DGDR) is shown in Fig. 5. The first data points above the (γ,n) threshold should not be considered because Γ_γ and Γ_n are of the same magnitude.

It should be noted that γ-ray strength functions deduced from the photoexcitation experiments are related to the target nucleus whereas strength functions obtained in neutron capture studies concern the residual nucleus. However, γ-ray strength functions are expected to change very slowly with mass number implying that comparisons between adjacent heavy nuclei are relevant.

Several conclusions can be drawn from the data presented in Fig. 5. The agreement between the extrapolation of the photonuclear data, the average reduced widths of high-energy primary transitions, and our results is quite good. Though special attention was devoted to a careful determination of the γ-ray spectrum shape in the low-energy region, the γ-ray strength function around 1.5 MeV is subject to uncertainties which are difficult to estimate. The minimum near 2.5 MeV seems to be real and the increase in $f(E_\gamma)$ below this energy may be due to $E2$ transitions.

In previous works the existence of a low-energy resonance in the γ-ray strength function, called the pigmy resonance, has been discussed. Compared to the extrapolation of the giant dipole resonance as calculated from the Lorentzian parameters, the strength function deduced in the present work departs significantly especially between 2 and 5 MeV. On the other hand, if the depression factor discussed above is used to fit the low-energy part of the giant resonance, there is a small strength excess around 5.5 MeV. The strong increase of the strength function between $E_\gamma = 3.5$ and 5.5 MeV and the much slower increase above 5.5 MeV are responsible for the 5.5 MeV bumps in the gamma-ray spectra. A similar situation is observed for thulium, as will be discussed later.

The total average radiative width at the neutron binding energy given by Eq. (4) has been calculated from the present results and from the giant dipole resonance parameters [Eq. (5)] using the two nuclear temperature values, $T = 0.71$ and $T = 0.74$ MeV. The calculated widths are compared with the experimental value[30] in Table IV. The error

TABLE IV. Average total radiative widths at the neutron binding energy.

Nucleus	T (MeV)	Γ_γ [a] (meV)	Γ_γ (GDR) (meV)	Γ_γ (DGDR) (meV)	Γ (meV)
^{104}Rh	0.752	184 ± 14	182	102	171 ± 3 [c]
	0.844	300 ± 20	317	181	
^{170}Tm	0.590	68 ± 5	83 [b]		84 ± 4 [d]
	0.625	86 ± 6	112 [b]		
^{198}Au	0.707	127 ± 13	418	102	125 ± 11 [e]
	0.735	153 ± 16	505	126	

[a] Present work.
[b] Computed using the ^{175}Lu GDR parameters.
[c] Reference 15.
[d] Reference 36.
[e] Reference 30.

in the calculated widths takes into account the uncertainty in the absolute value of the strength function along with the effect of the extrapolation below 1.5 MeV. The widths depend strongly on the level density as shown in Table IV. The deduced total average width for ^{198}Au is in agreement with the experimental value for $T = 0.71$ MeV, a temperature obtained using the rigid-body value of the moment of inertia of the nucleus. The widths computed from the extrapolation of the Lorentzian with parameters of Table III are about a factor of 4 too large. The use of the depression factor in the low-energy part of the giant resonance gives total widths in better agreement with the experimental value. The temperature $T = 0.75$ MeV used in previous works[25,26] would result in $\langle\Gamma_\gamma\rangle = 194$ meV if applied to our capture spectra.

B. Rhodium

The spectra from ^{103}Rh(n,γ) presented in Fig. 4 are exponential in shape. The deduced strength functions for the nuclear temperatures $T = 0.75$ and $T = 0.84$ MeV are presented in Fig. 7.

The giant dipole resonance parameters in ^{103}Rh have been determined by Leprêtre *et al.*[31] and are given in Table III. The data points below 10 MeV and the extrapolation of the curve fitting the dipole resonance are presented in Fig. 7 and compared to our results. However, for $E_\gamma < 13$ MeV, the experimental values fall below the calculated Lorentzian curve. A better agreement was obtained by multiplying this curve by a depression factor [Eq. (14)] with the parameters $\alpha = 0.060$ MeV^{-1} and $E_0 = 13.4$ MeV. The strength function corresponding to this depressed Lorentzian (DGDR) is also presented in Fig. 7. The energy dependence of these strength functions is in good agreement with our results.

Thermal neutron capture spectra obtained by Bartholomew *et al.*[32] show that transitions to states at about 1 and 2 MeV in excitation energy are enhanced compared to other transitions. The thermal capture cross section is dominated by a strong resonance at 1.257 eV and the γ-ray spectrum might be strongly influenced by the characteristics of this resonance.

The γ-ray strength function deduced from the resonance capture studies is obtained by averaging the γ-ray intensities I_γ over many neighboring resonances in order to reduce the Porter-Thomas fluctuations. An additional smoothing of these fluctuations can be achieved by averaging over several neighboring gamma rays.[2] This has been done by Rimawi *et al.*[33] Strong transitions were observed with relatively intense 6.0–6.2 MeV gamma rays. The reduced partial widths I_γ/E_γ^3 were summed over intervals of 200 keV and the strength function was deduced by multiplying with a constant temperature level density [Eq. (9)] with $T = 1.0$ MeV. It was then found that the strength function was constant in the range 4.7

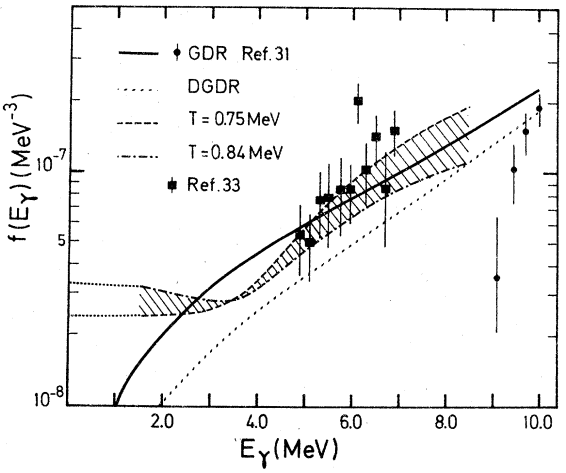

FIG. 7. Strength functions for ^{104}Rh compared to the photonuclear and the resonance averaged data.

$< E_\gamma < 7.0$ MeV. However, if the temperature $T = 0.8$ MeV deduced in the present work is used to determine the energy dependence of the level density, then the average partial radiation width is no longer following the E_γ^3 law. The energy dependence of this average reduced width is compared to our results in Fig. 7 where the data have been normalized to ours at $E_\gamma = 5$ MeV. The energy dependence is in good agreement with our strength function except for the peak at 6.1 MeV which was not observed in the present experiment.

The γ-ray spectra averaged over many resonances have also been measured by Haste and Thomas.[34] The averaged spectra show an enhancement in the 6.0–6.2 MeV region in agreement with the results of Rimawi *et al.*[33] The average correlation coefficient between reduced neutron widths and reduced partial radiation widths in the region of 6.0 MeV was found to be very small, in disagreement with the results of Rimawi *et al.*[33]

The total radiation widths at B_n have been calculated from our deduced strength functions and from the extrapolation of the giant dipole resonance by a Lorentzian and by a depressed Lorentzian. The results are given in Table IV. The experimental total width is in agreement with our data using the temperature $T = 0.75$ MeV whereas the extrapolation by the depressed Lorentzian agrees reasonably well with the strength function based on the temperature $T = 0.84$ MeV.

C. Thulium

A small bump around 3.5 MeV can be observed in the ^{169}Tm(n,γ) spectra of Fig. 4 for all neutron energies, except 3.0 MeV where it is masked by gamma rays from inelastic scattering. Strength function curves corresponding to the nuclear temperatures $T = 0.59$ and 0.63 MeV (Table II) are plotted in Fig. 8.

As the giant dipole resonance in thulium has not been investigated by photonuclear experiments, data obtained for nearby nuclei, namely ^{nat}Er and ^{175}Lu, have been used with the parameters[35] given in Table III. Data points and Lorentzian extrapolations are presented in Fig. 8 and compared with the γ-ray strength functions deduced from the present work. The agreement down to 1 MeV is fairly good.

The ^{169}Tm nucleus is in a region of deformed nuclei, where a bump in the capture spectrum is unexpected.[28] The bump in the capture spectrum is clearly reflected in the γ-ray strength function by a "resonance" around 3.5 MeV with a width of about 1.0 MeV.

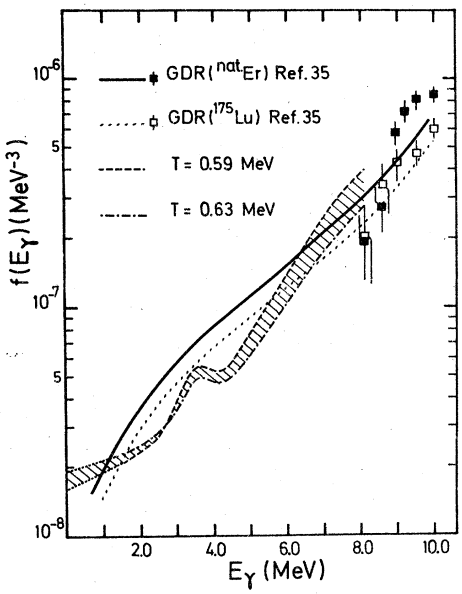

FIG. 8. Strength functions for ^{170}Tm compared to the γ-ray absorption cross sections in ^{nat}Er and ^{175}Lu.

Apart from strong transitions to levels around 0.6 MeV, a small bump was observed in thermal neutron capture[24] for gamma rays between 3.5 and 4.0 MeV in agreement with the bump position observed in the present work.

The total radiative widths computed from our results are presented in Table IV and compared with the measured value. The agreement is obtained with $T = 0.63$ MeV.

VI. DISCUSSION

The position of the bumps observed in the gold and thulium capture gamma-ray spectra was found to be independent of the initial excitation energy and cannot be explained as a direct capture effect. For neutron energies between 0.5 and 3.0 MeV, various partial waves up to $l = 3$ must be considered and then the intensity of the bump would change with excitation energy whereas the observed relative intensity of the bump is almost constant.

In a microscopic approach, the collective nature of the dipole state is expressed in terms of a coherent superposition of many 1p-1h $E1$ states. The incident neutron can excite neutron and proton particle-hole configurations of the type $(3p_{3/2}^{-1}4s_{1/2})$, $(2f_{5/2}^{-1}2g_{7/2})$, $(3p_{1/2}^{-1}3d_{3/2})$, and so on. In the lead region, the spacing between neighboring shells of opposite parity is about 5.5 MeV.[37] It is assumed that some of the $E1$ strength remains around 5.5 MeV and is not pushed up into the giant dipole resonance (GDR).

The experimental fact that part of the $E1$ strength

is left around the unperturbed particle-hole energy, in particular for nuclei in the vicinity of closed shells, is not yet understood. Efforts by several groups have, however, been put into the problem and a short review of the most promising recent developments is given below.

The basic mechanism of dipole absorption in nuclei has been considered as a collective vibration of neutrons against protons, and the hydrodynamical model[38] was able to describe the general features of the giant dipole resonance. A three-fluid model predicting low-energy resonances containing 1 to 5% of the giant dipole strength has also been developed.[39] Calculations for ^{208}Pb led to a giant resonance at 13 MeV and a pigmy resonance around 4.5 MeV. However, these results depend on several parameters and the separation of the neutron fluid into two parts is quite arbitrary.

The distribution of dipole strength in ^{132}Sn and ^{208}Pb has been investigated by Harvey and Khanna[40] in the framework of the schematic model of Goswami and Pal.[41] In ^{208}Pb for example, the calculations with Gaussian radial integrals and realistic particle-hole energies showed that about 5% of the dipole strength was collected into two regions around 4.5 and 7.0 MeV. The remaining 95% strength was collected among four states above 10.5 MeV, one of them containing about 75% of the total strength. This decoupling from the giant dipole resonance into the low-energy region is due to the differences in residual interaction radial integrals. On the other hand, the relocalization of the strength into miniresonances depends on the mean energy differences between neutron and proton particle-hole states.

The miniresonances were found[42] to appear in mass-number regions where s- or p-neutron single-particle binding energies are near zero. The decoupling from the GDR appears at energies close to the unperturbed energies of particle-hole states involving the s- or p-neutron states. This effect has been investigated by Gyarmati *et al.*[43] Recent calculations have been made by Csernai *et al.*[44] for ^{116}Sn where the p-neutron states are near threshold. Depending on the range of the two-body force, about 5% of the total transition rate has been found in the 6–9 MeV energy region.

VII. SUMMARY

The present paper reports on neutron capture experiments designed to determine the gamma-ray strength function in the energy region below the giant dipole resonance for ^{104}Rh, ^{170}Tm, and ^{198}Au. The gamma-ray strength functions were determined by the spectrum fitting method and the crucial point in the analysis is the treatment of level densities. The results are in general agreement with data obtained by the same or other techniques. The gamma-ray strength function for ^{104}Rh varies smoothly with energy. For ^{170}Tm and ^{198}Au, on the other hand, bumps in the strength functions at 3.5 and 5.5 MeV, respectively, are required to describe the observed gamma-ray distributions. It is interesting to note that for near closed-shell nuclei, Rh and Au, the measured average total radiative widths are well accounted for by a strength function calculated with the level-density parameter T corresponding to the rigid-body moment of inertia. For the deformed nucleus Tm, on the other hand, the use of a T value corresponding to half the rigid-body moment of inertia gives a better agreement with the measured data.

ACKNOWLEDGMENTS

We wish to thank Dr. I. Bergqvist for continued interest and encouragement during the course of this work. We also appreciate the assistance of Dr. M. A. Lone who suggested the new method of summing levels. We wish to acknowledge also the continued support and encouragement of Dr. A. Michaudon. Two of us (D.D. and L.N.) greatly appreciate the hospitality shown us by the staff of the Service de Physique Nucléaire de Bruyères-le-Châtel.

---

*Permanent address: Los Alamos Scientific Laboratory, Los Alamos, N.M.

†Permanent address: Tandem Accelerator Laboratory, Uppsala, Sweden.

[1]G. R. Satchler, Phys. Rep. 14C, 97 (1974).

[2]G. A. Bartholomew, E. D. Earle, A. J. Ferguson, J. W. Knowles, and M. A. Lone, Adv. Nucl. Phys. 7, 229 (1973).

[3]J. M. Blatt and V. E. Weisskopf, *Theoretical Nuclear Physics* (Wiley, New York, 1952).

[4]P. Axel, Phys. Rev. 126, 671 (1962).

[5]D. M. Brink, Ph.D. thesis, Oxford, 1955.

[6]S. Joly, J. Voignier, G. Grenier, D. M. Drake, and L. Nilsson, Nucl. Sci. Eng. 70, 53 (1979).

[7]S. Joly, J. Voignier, G. Grenier, D. M. Drake, and L. Nilsson, Nucl. Instrum. Methods 153, 493 (1978).

[8]J. L. Leroy, J. L. Huet, and J. Gentil, Nucl. Instrum. Methods 88, 1 (1970).

[9]N. Starfelt, Nucl. Phys. 53, 397 (1964).

[10]E. S. Troubetzkoy, Phys. Rev. 122, 212 (1961).

[11]A. Gilbert and A. G. W. Cameron, Can. J. Phys. 43, 1446 (1965).
[12]W. Dilg, W. Schantl, H. Vonach, and M. Uhl, Nucl. Phys. A217, 269 (1973).
[13]M. Bormann, H. H. Bissem, E. Magiera, and R. Warnemünde, Nucl. Phys. A157, 481 (1970).
[14]L. E. Samuelson, W. H. Kelly, R. L. Auble, and W. C. McHarris, Nucl. Data Sheets 18, 125 (1976).
[15]P. Ribon, J. Girard, and J. Trochon, Nucl. Phys. A143, 130 (1970).
[16]M. R. Schmorak and R. L. Auble, Nucl. Data Sheets 15, 371 (1975).
[17]S. de Barros, V. D. Huynh, J. Julien, J. Morgenstern, and C. Samour, Nucl. Phys. A131, 305 (1969).
[18]B. Harmatz, Nucl. Data Sheets 21, 377 (1977).
[19]J. S. Desjardins, J. L. Rosen, W. W. Havens, Jr., and J. Rainwater, Phys. Rev. 120, 2214 (1960).
[20]R. N. Alves, J. Julien, J. Morgenstern, and C. Samour, Nucl. Phys. A131, 450 (1969).
[21]M. A. Lone, private communication.
[22]M. Maruyama, Nucl. Phys. A131, 145 (1969).
[23]B. Lundberg and N. Starfelt, Nucl. Phys. 67, 321 (1965).
[24]L. V. Groshev, A. M. Demidov, V. I. Pelekhov, L. L. Sokolovskii, G. A. Bartholomew, A. Doveika, K. M. Eastwood, and S. Monaro, Nucl. Data Tables A5, 243 (1969).
[25]E. D. Earle, M. A. Lone, G. A. Bartholomew, W. J. McDonald, K. H. Bray, G. A. Moss, and G. C. Neilson, Can. J. Phys. 52, 989 (1974).
[26]E. D. Earle, I. Bergqvist, and L. Nilsson, A. B. Atomenergi Report No. AE-515 (1977).
[27]G. D. Loper, L. M. Bollinger, and G. E. Thomas, Argonne Report No. ANL-7971 (1972).
[28]G. A. Bartholomew, I. Bergqvist, E. D. Earle, and A. J. Ferguson, Can. J. Phys. 48, 687 (1970).
[29]A. Veyssière, H. Beil, R. Bergère, P. Carlos, and A. Leprêtre, Nucl. Phys. A159, 561 (1970).
[30]J. Julien, S. de Barros, G. Bianchi, C. Corge, V. D. Huynh, G. Le Poittevin, J. Morgenstern, F. Netter, C. Samour, and R. Vastel, Nucl. Phys. 76, 391 (1966).
[31]A. Leprêtre, H. Beil, R. Bergère, A. De Miniac, A. Veyssière, and K. Kernbach, Nucl. Phys. A219, 39 (1974)
[32]G. A. Bartholomew, A. Doveika, K. M. Eastwood, S. Monaro, L. V. Groshev, A. M. Demidov, V. I. Pelekhov, and L. L. Sokolovskii, Nucl. Data Tables A3, 367 (1967).
[33]K. Rimawi, J. B. Garg, R. E. Chrien, and R. G. Graves, Phys. Rev. C 2, 1793 (1970).
[34]T. J. Haste and B. W. Thomas, J. Phys. G 1, 981 (1975).
[35]R. Bergère, H. Beil, P. Carlos, and A. Veyssière, Nucl. Phys. A133, 417 (1969).
[36]S. F. Mughabghab and D. I. Garber, Report No. BNL-325 (1973).
[37]R. A. Moyer, B. L. Cohen, and R. C. Diehl, Phys. Rev. C 2, 1898 (1970).
[38]V. Rezwani, G. Gneuss, and H. Arenhövel, Nucl. Phys. A180, 254 (1972).
[39]R. Mohan, M. Danos, and L. C. Biedenharn, Phys. Rev. C 3, 1740 (1971).
[40]M. Harvey and F. C. Khanna, Nucl. Phys. A221, 77 (1974).
[41]A. Goswami and M. K. Pal, Nucl. Phys. 35, 544 (1962).
[42]A. M. Lane, Ann. Phys. (N.Y.) 63, 171 (1971).
[43]B. Gyarmati, A. M. Lane, and J. Zimanyi, Phys. Lett. 50, 136 (1974).
[44]L.P. Csernai, J. Zimanyi, B. Gyarmati, and R. G. Lovas, Nucl. Phys. A294, 41 (1978).